The Journal of Experimental Biology 203, 3279–3287 (2000)
Printed in Great Britain © The Company of Biologists Limited 2000
JEB2728

ELECTRORECEPTION IN *GYMNOTUS CARAPO*: PRE-RECEPTOR PROCESSING AND THE DISTRIBUTION OF ELECTRORECEPTOR TYPES

MARÍA E. CASTELLÓ, PEDRO A. AGUILERA, OMAR TRUJILLO-CENÓZ AND ANGEL A. CAPUTI*

Departamento de Neuroanatomía Comparada, Instituto de Investigaciones Biológicas Clemente Estable, Avenida Italia 3318, CP 11600, Montevideo, Uruguay

*Author for correspondence (e-mail: angel@iibce.edu.uy)

Accepted 28 July; published on WWW 9 October 2000

Summary

This paper describes the peripheral mechanisms involved in signal processing of self- and conspecific-generated electric fields by the electric fish *Gymnotus carapo*. The distribution of the different types of tuberous electroreceptor and the occurrence of particular electric field patterns close to the body of the fish were studied. The density of tuberous electroreceptors was found to be maximal on the jaw (foveal region) and very high on the dorsal region of the snout (parafoveal region), decaying caudally. Tuberous type II electroreceptors were much more abundant than type I electroreceptors. Type I electroreceptors occurred exclusively on the head and rostral trunk regions, while type II electroreceptors were found along as much as 90 % of the fish. Electrophysiological data indicated that conspecific- and self-generated electric currents are 'funnelled' by the high conductivity and geometry of the body of the fish. These currents are concentrated at the peri-oral zone, where most electroreceptors are located. Moreover, within this region, field vector directions were collimated, constituting the most efficient stimulus for electroreceptors. It can be concluded that the passive properties of the fish tissue represent a pre-receptor device that enhances exafferent and reafferent electrical signals at the fovea–parafoveal region.

Key words: electric fish, *Gymnotus carapo*, electric image, electroreception, electroreceptor innervation, electric organ discharge waveform, fovea, gymnotiform, lateral line, pre-receptor processing.

Introduction

Electric fish have evolved electrosensory systems to communicate and to explore their environment. Transcutaneous current density is the specific stimulus for these systems. Objects and electrical discharges from conspecifics cause changes in the pattern of transcutaneous current density. These changes constitute the so-called physical electric images (Bastian, 1986; Caputi et al., 1998; Budelli and Caputi, 2000). Objects and electrical signals from conspecifics are represented by the activity of different electroreceptor populations and also by the pattern of discharge of primary afferent fibres. These patterns of activity may be defined as the first neural electric image. The transformation of physical images into neural images depends both on the distribution of electroreceptors and on their individual responses to local transcutaneous currents.

In pulse-type gymnotids, the skin contains various types of electroreceptor sensitive to amplitude, frequency and phase modulations of the temporal waveform of local transcutaneous currents (Bullock, 1982; Watson and Bastian, 1979). Studies concerned with the distribution of anatomical and functional types of electroreceptors and their central representation indicate a heterogeneous spatial sampling of the electric image (Szabo, 1965; Westby, 1975; Heiligenberg and Dye, 1982; Shumway, 1989a,b; Yager and Hopkins, 1993).

Detailed information concerning the spatial distribution of electroreceptors in *Gymnotus carapo* is lacking, so we have studied this subject using a variety of technical approaches. The present paper provides evidence that there is a foveal–parafoveal region on the rostral pole of the fish body exhibiting a high concentration of various types of electroreceptor. This array of electroreceptors is innervated by the main branches of two of the largest nerves in the fish (the mandibular nerve and the supraorbital nerve), which in turn project onto a large area of the electrosensory lobe (Castelló et al., 1998). In addition, pre-receptor processing of exafferent and reafferent electrical signals at the foveal–parafoveal region is demonstrated.

Materials and methods

Fifty *Gymnotus carapo* Linn. were used in this study. Fish lengths ranged between 2.5 and 80 cm, and included both juvenile and adult animals. Fish were collected following the rules of División Fauna of the Ministerio de Agricultura y Pesca, Uruguay. All surgery was performed under cold anaesthesia. Experiments were performed under the surveillance of the committee for the use of experimental

animals of the Instituto de Investigaciones Biológicas Clemente Estable and fulfilled the guidelines of the Society for Neuroscience.

Histological procedures

Samples of skin (2 mm×4 mm×0.3 mm) were removed from formaldehyde-fixed animals using a scalpel (jaw, *N*=25; dorsum of the snout, *N*=7; dorsum of the trunk at 10 %, 25 % and 50 % of fish length measured from the snout, *N*=7). In six fish, the skin of the whole head was carefully removed and divided into two pieces, one corresponding to the dorsal region of the snout and the other to the jaw. The pieces of skin were mounted in saline and observed using a light microscope connected to a television camera and printer. This procedure allowed a clear visualisation and identification of ampullary and tuberous receptors. Printer images obtained at low magnification were mounted together to reconstruct the whole area of skin. A grid of unit size equivalent to 0.25–4 mm^2 of skin was projected onto the pictures, and the electroreceptor density for each unit was calculated by dividing the number of receptors by the size of the unit. The data were interpolated and represented as contour isodensity lines.

Two methods were used to study electroreceptor innervation. (i) Sudan techniques were used for staining whole flat mounts, in which the myelinated nerve branches are clearly stained. The preparations were cleared and mounted in Apathy's medium containing sucrose and gum arabic (Carazzi and Levi, 1916). (ii) A silver impregnation technique (Ramon y Cajal and de Castro, 1933) revealed the unmyelinated terminal branches contacting the receptor cells. Micrographs were taken at different magnifications using black-and-white or fine-grain colour film.

In three fish, the mandibular and supraorbital nerve branches of the lateral-line nerve were dissected; hand drawings were made using a *camera lucida* attached to the dissecting microscope.

Electrophysiological recordings

The self-generated electric organ discharge (EOD)-associated field and the conspecific EOD-associated field occurring near the electroreceptive surface of a fish (the receptor fish) were investigated in 10 fish. The receptor fish was restrained using a net in the center of a tank (32 cm×21 cm×10 cm) filled with tap water (220–240 $\mu S\ cm^{-1}$). A conspecific fish (the emitting fish), restrained in another net, was placed parallel to the receptor fish, 8–10 cm away. Self-generated EOD- and conspecific-associated fields were recorded close to the skin of the receptor fish, at the head and along the dorsal region of the trunk. Conspecific-associated fields were compared with two additional field recordings made at the same spatial coordinates: (i) after removing the receptor fish from the aquarium and (ii) after substituting the receptor fish body with a tapered iron bar with one blunt and one sharpened edge.

Local waveforms of the EOD-associated fields were recorded and processed using four electrodes assembled into a single probe (Fig. 1). The probe was constructed using four 200 μm nichrome wires isolated except at the tip (impedance approximately 50 kΩ). The tip of one wire (the reference electrode) was located near the intersection of the three others (active electrodes). The reference electrode was located close to the skin. The active electrodes were oriented along orthogonal axes (rostro-caudal, dorsal-ventral and medial-lateral) with their tips 2 mm from the intersection point (Fig. 1). The electric field voltage difference between each of the active electrodes and the reference electrode was recorded with a high-input-impedance, high-gain differential amplifier. Raw data were transformed into orthogonal components by correcting for the eccentricity of the reference electrode. The resultant field vector was calculated from these components. As shown in Fig. 1, the magnitude and orientation of the field vector are functions of time.

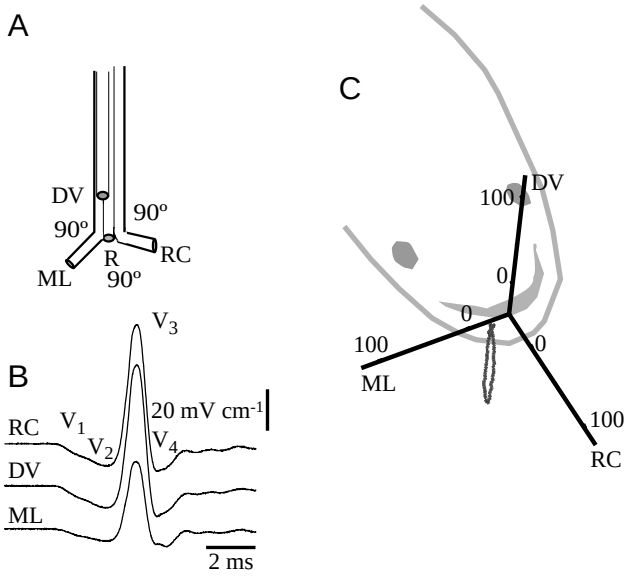

Fig. 1. Recording procedure. (A) The assembly of three active electrodes oriented along orthogonal axes (RC, rostro-caudal; DV, dorso-ventral; ML, medio-lateral) with their tips 2 mm from their intersection approximately where the fourth reference electrode (R) was located. (B) Local electric organ discharge fields (LEOD) along the three axes of the probe. The four components of the LEOD are indicated as V_1, V_2, V_3 and V_4. (C) Three-dimensional representation of the field vector trajectory (elliptical shape) referred to the recording site on the head of the fish. Values are $mV\ cm^{-1}$.

To make a detailed study of the field around the receptor fish and to compare it with the field generated by the emitter fish in a homogeneous medium, a second set of recordings was performed using the same methodology in a large tank (50 cm×50 cm×5 cm, *N*=3). In this case, a horizontal surface (8 cm×18 cm), centred on the receptor fish, was explored, and the field recordings were compared with recordings made at the same coordinates after removing the receptor fish from the tank. Electrodes were placed sequentially along five equally spaced lines parallel to the longitudinal axis of the receptor fish (from 4 cm rostral to 14 cm caudal of the head, every 2 cm).

Results

Distribution of electroreceptor types on the fish skin

As described previously (for a review, see Szabo, 1974), we have identified two main types of electroreceptor: (i) tuberous and (ii) ampullary. The tuberous receptors can be further subdivided into two main types in gymnotid fish (Szabo, 1974). Type I is characterised by the occurrence of symmetrical myelinated preterminal nerve branches and type II by randomly branched unmyelinated preterminal nerve branches (Fig. 2).

Echagüe and Trujillo-Cenóz (1980) confirmed the basic patterns reported by Szabo (1974), and also described subtypes within the basic type I electroreceptor: subtype α, with numerous long myelinated preterminal branches, and subtype β, with only one or two myelinated preterminal branches. Both Szabo (1974) and Echagüe and Trujillo-Cenóz (1980) also differentiate two subtypes of type II tuberous electroreceptor: subtype γ (type IIB of Szabo, 1974), characterised by the occurrence of a double group of long unmyelinated branches, and subtype δ (type IIA of Szabo, 1974), characterised by a single group of short unmyelinated branches. There is no clear correlation between these morphological subtypes within types I and II and stimulus coding properties, so we have focused on the distribution of tuberous electroreceptor types I and II and disregarded the different branching patterns within each type. Types I and II (Fig. 2) electroreceptors have been correlated with the functional types M (pulse marker units) and B (burst duration coders), the origins of the fast and slow electrosensory pathways, respectively (Bullock, 1982; Szabo, 1974; Szabo et al., 1975; Zakon, 1986).

Measurements of electroreceptor organ diameters showed that typical type I tuberous electroreceptors were 1.55 times larger in diameter than typical type II tuberous electroreceptors (106±7 μm and 68±9 μm respectively, means ± S.D., N=18 for each type, fish length 9.5 cm). These measurements were made in silver-impregnated material that allowed us a clear visualisation of the branching pattern. However, there were also intermediate types with characteristics common to both type I and type II electroreceptors. These were not taken into account in the statistical analyses. However, they were inevitably counted when employing methods that did not reveal the afferent fibre terminal branches (non-stained and Sudan-black-stained preparations).

Sudan black staining revealed that electroreceptor diameter was correlated with the diameter of their afferent fibres (Fig. 3). This result is consistent with the finding of Szabo (1974) that type I tuberous electroreceptors are connected to nerve fibres of large diameter, while type II tuberous electroreceptors are connected to nerve fibres with a relatively small diameter. Tuberous type I and II electroreceptors may represent the extremes of a continuum with intermediate forms, as suggested by Viancour (1979). Our data from Sudan-stained preparations were more consistent with a continuum than a dichotomy of electroreceptor types. However, this question remains unresolved because the branching pattern within the organ cannot be identified in this kind of material.

Regardless of the technical procedure used, maximum tuberous electroreceptor density occurred on the ventral surface of the most rostral regions of the head, constituting a kind of fovea. Another high-density zone of electroreceptors was found on the dorsal surface of the head (snout), which we

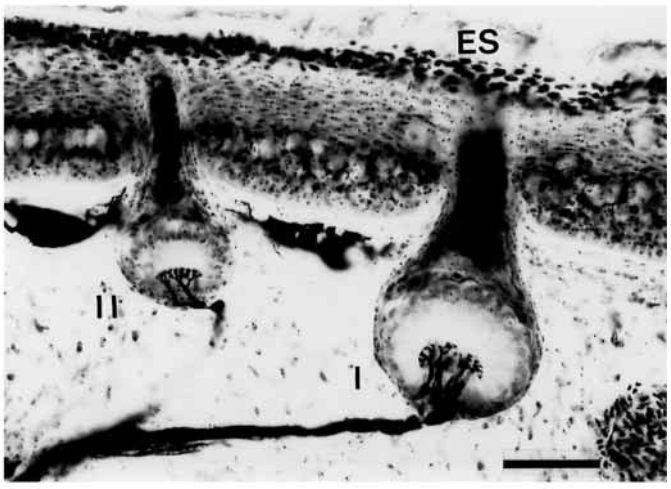

Fig. 2. Micrograph of a transverse section through the skin on the head of *Gymnotus carapo*. This reduced silver-stained preparation shows the two main types of tuberous electroreceptor found in this species: types I and II. Note that type I electroreceptors (I) have long thick terminal nerve branches penetrating a large-diameter organ that protrudes deep into the corion. Type II tuberous electroreceptors (II) have short thin terminal nerve branches that innervate a small-diameter organ. Scale bar, 50 μm. ES, epidermal surface.

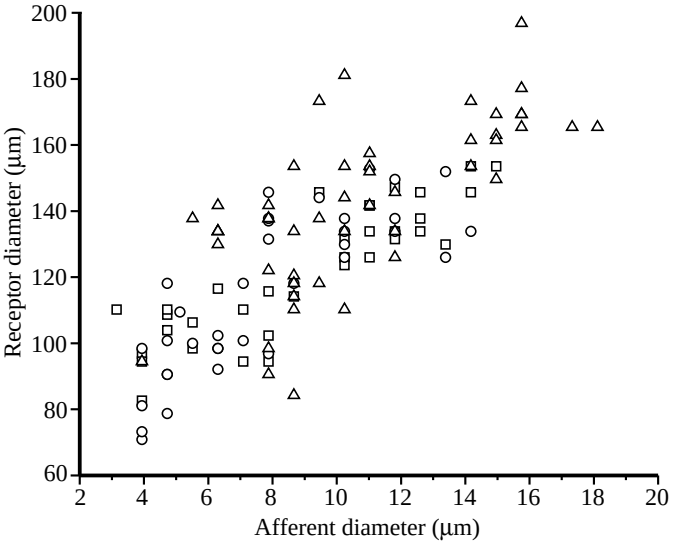

Fig. 3. Plot of the diameter of tuberous electroreceptors as a function of afferent fibre diameter. Data from three fish of different lengths (7.5 cm, open squares, N=34; 13.5 cm, open circles, N=35; and 20 cm, open triangles, N=51). Data were pooled for linear correlation analysis: N=120; r=0.8 P<0.0001. Note that this plot contains information from three populations of tuberous electroreceptors, without type identification.

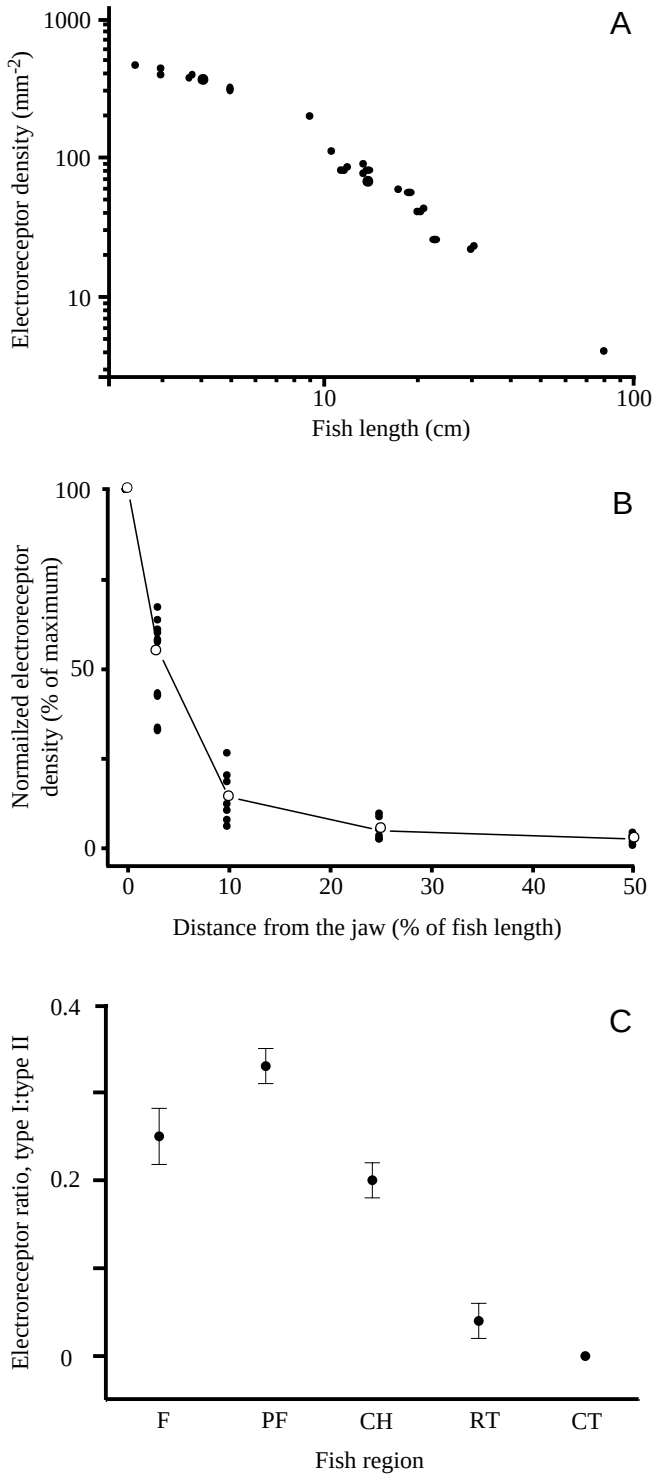

Fig. 4. (A) Tuberous electroreceptor density at the fovea as a function of fish length. Density is expressed as the maximal number of receptors per mm^2 (N=25). (B) Distribution of tuberous electroreceptors along the length of the fish. Plot of the normalized electroreceptor density (expressed as a percentage of the maximum) as a function of the normalized distance from the snout (expressed as a percentage of fish length). Open circles, mean values for seven specimens; filled circles, values from seven individuals ranging from 9 to 30 cm in length. (C) Ratio of the number of type I to type II tuberous electroreceptors at different locations along the body of the fish. Transverse sections passing through the fovea (F, N=27), parafovea (PF, N=27), caudal head (CH, N=22), rostral trunk (RT, N=14) and caudal trunk (CT, N=14) were obtained from one fish and examined under the microscope to identify and count type I and type II electroreceptors. Because the perimeters differed among sections, the most reliable method of quantifying density differences between the two electroreceptor types was to express the results as the ratio of the total number of type I electroreceptors to the total number of type II electroreceptors. Values are means ± S.D.

considered to be a parafovea. The electroreceptor density diminished rapidly rostro-caudally. Although the absolute density of tuberous electroreceptors decreases as the fish gets longer (Fig. 4A), when electroreceptor density was normalised to the maximum absolute value, this function was similar for fish ranging from 9 to 30 cm in length (Fig. 4B). The density of both tuberous electroreceptor types decreased as a function of the distance from the rostral pole, but at different rates for the two types. The ratio of type I/type II electroreceptors was approximately 1/4 at the foveal region, 1/3 at the parafoveal region and 1/5 at the caudal limit of the head; caudal to the origin of the anal fin, the ratio decayed to zero (Fig. 4C). Type II electroreceptors were found along as much as 90 % of the fish length.

A more detailed analysis of the distribution of tuberous electroreceptor density was performed in the head region. Fig. 5 shows electroreceptor density contour curves plotted for the dorsal surface of the head (the snout) (Fig. 5A) and for the mandibular region (Fig. 5B) in a fish 12 cm in length. Notwithstanding the dependence of the absolute receptor density on fish length, contour curves for fish of different lengths look similar when normalised to the maximum electroreceptor density. To facilitate correlation between the electroreceptor distribution data and the gross anatomy of the fish, we used the pores of the lateral-line canals as landmarks. In the mandibular region, the most rostral medial pore was numbered 0, while the others, with bilateral symmetry, were numbered in the rostral–caudal direction from 1 to 7. On the dorsal surface of the head, all lateral-line pores showed bilateral symmetry and were numbered from 1 to 9. In the mandibular region, maximum electroreceptor density occurred near the midline neighbouring pores 0, 1 and 2 (Fig. 5B). Electroreceptor density decayed along the rostro-caudal and latero-medial directions. Along the midline, receptor density fell to very low values at the level of pores 4 or 5. In the dorsal region, the electroreceptor density had two symmetrical relative maxima close to the mouth opening and pores 2 and 3 (Fig. 5A). However, maximal dorsal density was approximately 50 % of the maximum density in the mandibular region.

The branching pattern of mandibular and supraorbital nerves

After emergence from the lateral-line ganglion, the afferent fibres that innervate the electroreceptors of the head are segregated into three main branches: the mandibular, supraorbital and infraorbital nerves.

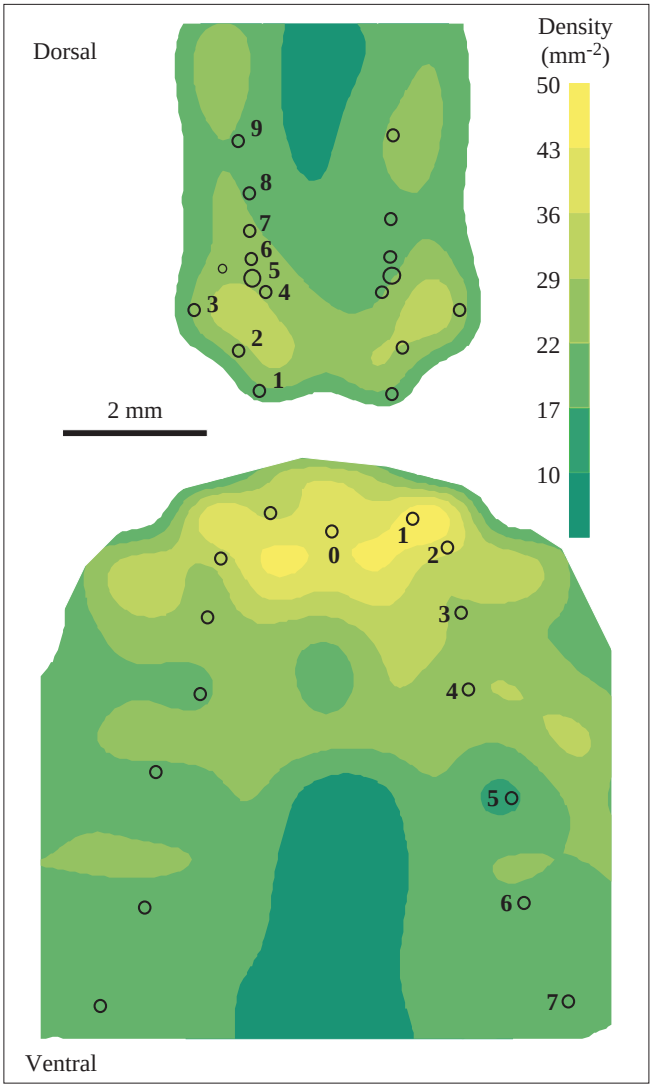

Fig. 5. Electroreceptor density contour curves illustrating the distribution of electroreceptors in the dorsal (top) and ventral (bottom) perioral regions in a 12 cm fish. Numbers 1–9 for the dorsal region and 0–7 for the mandibular region indicate the locations of the openings of the lateral line canals. The scale shows the number of electroreceptors per mm^2.

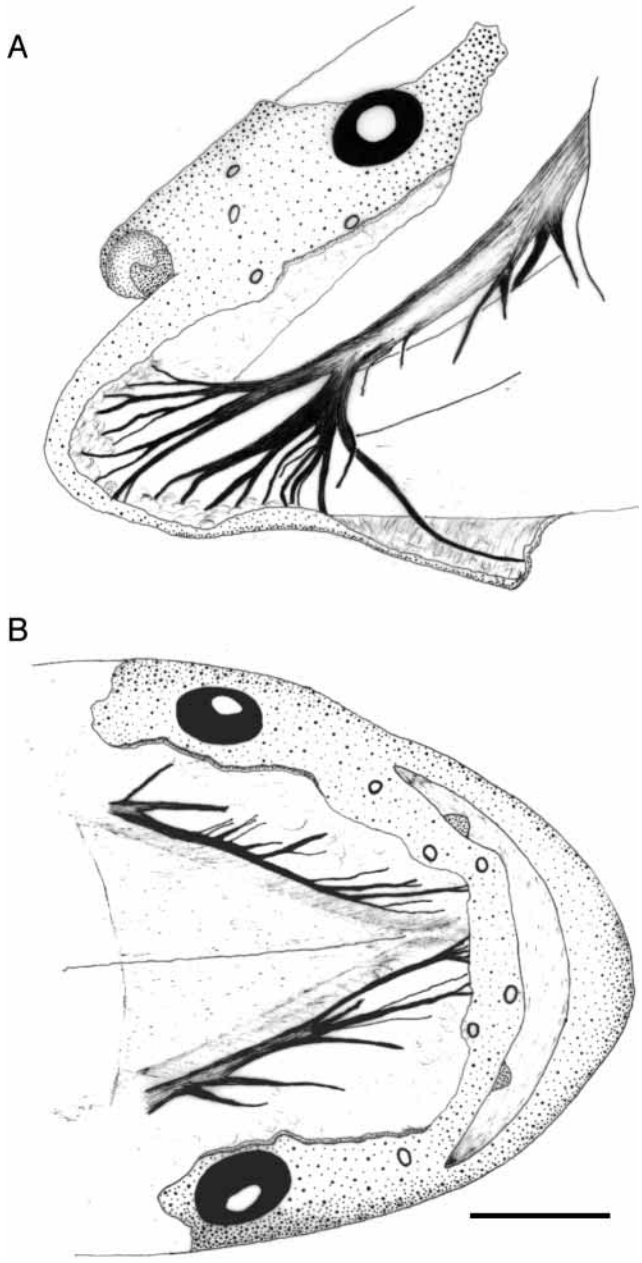

Fig. 6. Branching pattern of the mandibular (A) and supraorbital (B) nerves. Both nerves innervate electroreceptors in the dorsal and ventral regions of the head, respectively. The thicker nerve trunks innervate the most rostral regions with highest electroreceptor densities. Scale bar, 2 mm.

The mandibular nerve lies contiguous to the mandibular bone, giving rise to thin branches that innervate the lateral regions of the head and the caudal regions of the jaw. The bulk of mandibular nerve fibres continue up to the fovea, where they give rise to various thin nerve branches that emerge radially (Fig. 6A). These thin branches cross the sheet of dense connective tissue separating the skin from the muscle and the bone. The supraorbital nerve runs rostrally, attached to the ridge of the skull, and gives rise to several thin branches that innervate the skin around the eyes, the nerves finally dividing into several branches that innervate the parafovea (Fig. 6B).

In most cases, afferent fibres of tuberous type I electroreceptors followed a straight trajectory up to the receptor. In contrast, afferent fibres of type II electroreceptors and ampullary receptors ran up to the basal lamina and then parallel to the skin surface, beneath the melanocytes, before reaching their receptor.

Self-generated and conspecific-generated local fields at different sites on the skin

The local field (LEOD) associated with the self-generated EOD was 5–10 times larger than the LEOD generated by an

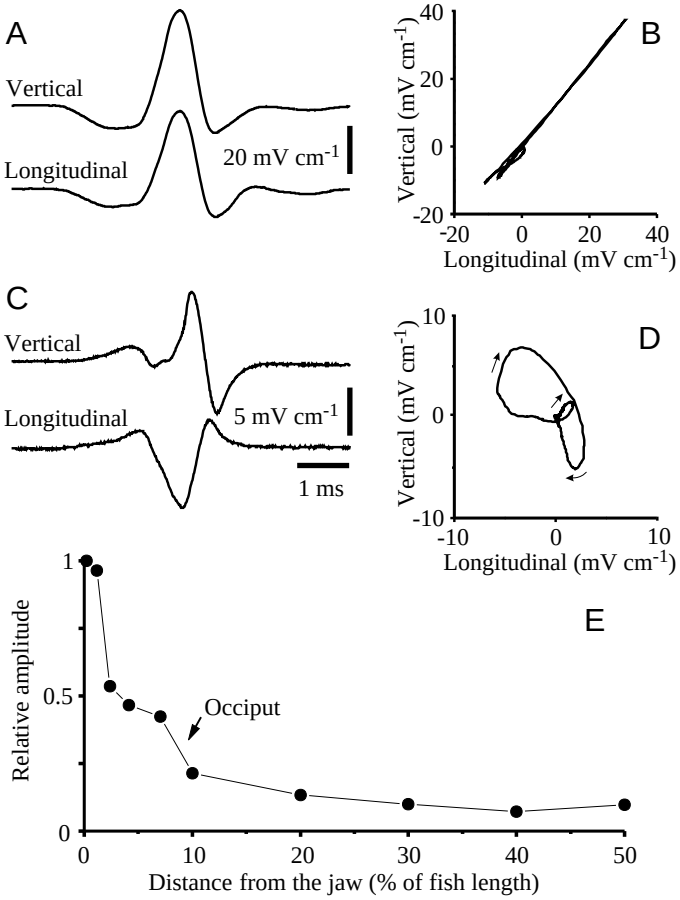

Fig. 7. Local fields associated with the self-generated electric organ discharge (LEOD) at the fovea (A,B) and on the trunk (C,D). LEODs were recorded with vertical and longitudinal orthogonal electrodes in the sagittal plane (A,C). The resulting field vectors were obtained by plotting the vertical field vectors as functions of the longitudinal vectors (B,D). Note that, at the fovea, the waveforms of the vertical and longitudinal components are similar (A), and current therefore flows along the same line throughout the OED (B). In contrast, on the trunk, the waveforms of the vertical and longitudinal components differ (C), and the current vectors therefore describe a loop (the sense of rotation is indicated by arrowheads) (D). The vector amplitude diminished from head to tail (E).

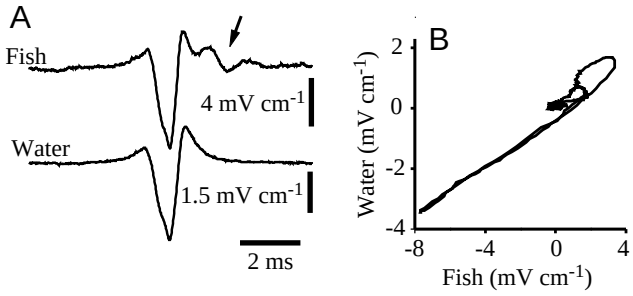

Fig. 8. (A) Local fields associated with the self-generated electric organ discharge (LEOD) from an emitting *Gymnotus carapo* recorded at the fovea of a receptor fish located in the middle of a 32 cm×21 cm×10 cm tank (top trace). The distance between the two fish was 10 cm. When the receptor fish was removed from the aquarium and field recordings were then made at the same site, the amplitude of the field decayed 2.5-fold (bottom trace). (B) The linear relationship between the two recordings indicates that there is no deformation of the LEOD waveform. Note that the main difference in waveform occurs in the decaying face of the V_4 component of the electric organ discharge (arrow). This late potential was associated with receptor activity since it disappeared when the receptor fish was removed from the tank.

emitting fish located 8 cm away from and parallel to the receptor fish.

On the head, the three orthogonal components of the self-generated LEOD showed closely similar waveforms. In addition, it was found that the angle of the field vectors with regard to the skin surface remained almost constant throughout the EOD (Fig. 7A,B). In contrast, on the trunk, the orthogonal components of the current density vectors differed, and the angle of the current density vector changed during the EOD, reflecting the different spatial origin of the EOD components (Fig. 7C,D). This kind of analysis also revealed that the amplitude of the vector at the foveal region was approximately five times larger than the amplitude of the vector at the trunk region (Fig. 7E).

The LEOD generated by a conspecific placed parallel, head to head or head-to-tail with and 8–10 cm away from the receptor fish was always larger on the fovea than at the trunk. Even though this LEOD was smaller than the self-generated LEOD, it was large enough to evoke a response in the receptor fish (Fig. 8A, arrow). This LEOD at the fovea was compared with the field recorded at the same spatial coordinates after removing the receptor fish from the tank. The LEOD at the fovea of the receptor fish was always larger than the field in the absence of the fish, suggesting that the LEOD is enhanced by the presence of the body of the receptor fish. As shown in Fig. 8B, the size of the LEOD waveform was proportional to the emitter-EOD-associated field recorded at the same coordinates after removing the fish from the aquarium. The small loop in Fig. 8B corresponds to the absence of biological responses in absence of the receptor fish. The gain of this mechanism (i.e. the slope of the line in Fig. 8B) depended on sizes of the fish and on their relative positions (range 1.3–4.5). The same kind of enhancing effect was obtained when the experiment was repeated using an iron bar instead of the receptor fish. The bar had a blunt and a sharpened end. The gain was 9.5 for the blunt end and 18 for the sharpened end. This supports the hypothesis that the body of the receptor fish ‘funnels’ currents because of its relatively large conductivity and elongated shape.

To investigate such pre-receptor effects further, we recorded the EOD field of the emitter fish in a larger tank in the presence and in the absence of the receptor fish. Fig. 9A shows a two-dimensional representation of the electric field of a fish (10 cm length) at the peak of the V_3 component of the EOD (black vectors). As mentioned above, the region investigated was a rectangle (8 cm×18 cm) with its major sides parallel to the

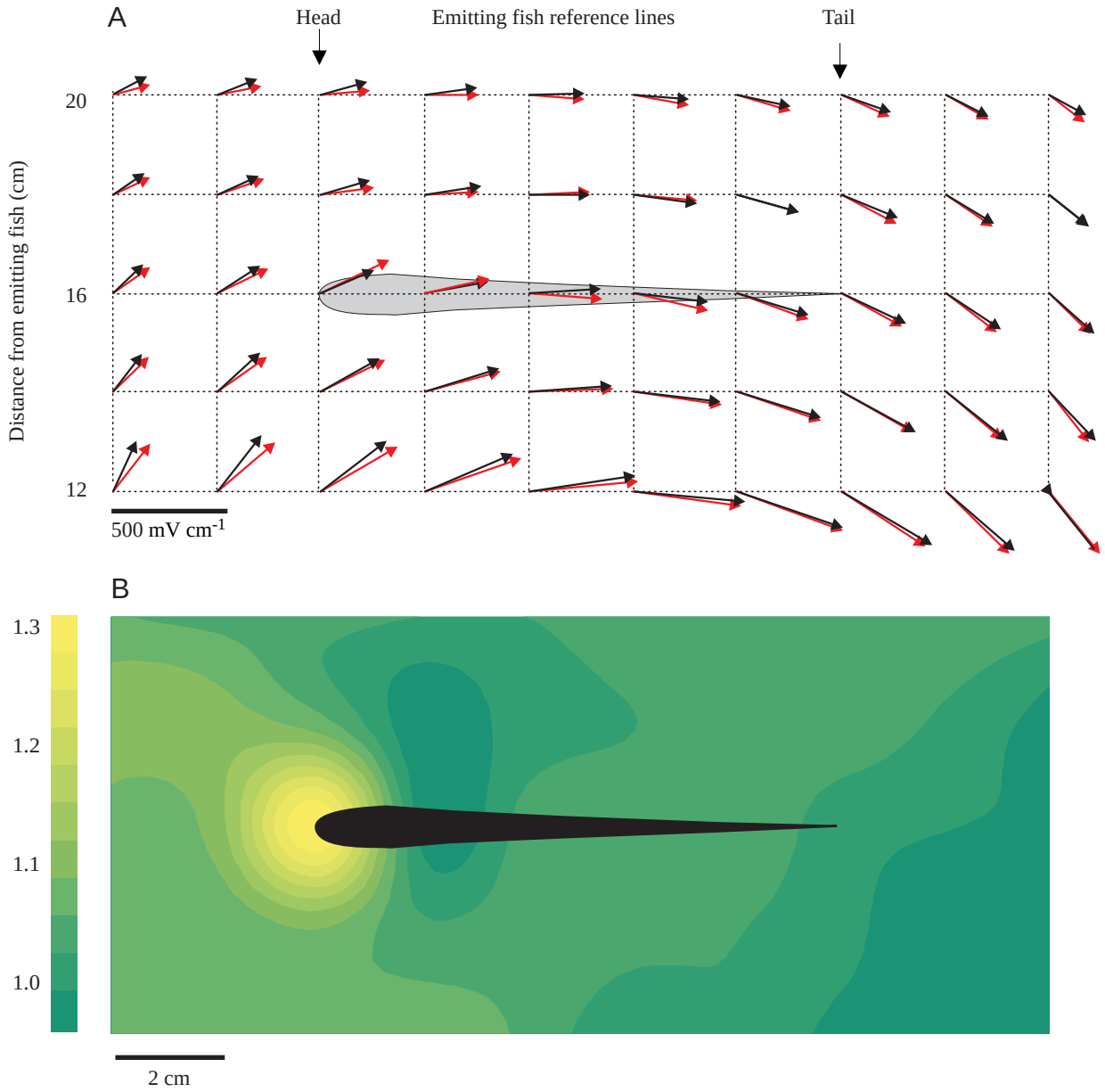

Fig. 9. The 'funnelling effect' of the body of the fish. (A) The two-dimensional electric field of a fish at the peak of the V_3 element of the electric organ discharge represented as gradient vectors in a rectangular region (18 cm×8 cm). Black vectors correspond to the field in water alone. After the introduction of a conspecific into the aquarium, the field is changed by the presence of the conductive tissues of the body of the second fish (red vectors). (B). The ratio of the amplitude of V_3 with a fish present to the amplitude of V_3 in the absence of a fish shown as a contour plot. It is evident that the largest change occurs at the head (yellow area). The emitting and receptor fish were both 10 cm long.

longitudinal axis of the emitter fish (12 and 20 cm apart) and its minor sides 4 cm rostral to the head and 4 cm caudal to the tail. The amplitude and direction of the field were modified after a conspecific had been introduced into the centre of the region under examination (red vectors). Fig. 9B shows, in a contour plot, the ratio between the vector amplitudes ('with fish' divided by 'without fish') and illustrates clearly that the largest change occurred at the head (yellow area). It is also important to note that, even when the fish were relatively far apart, the field at the fovea was always larger than at other sites along the receptor fish.

Discussion

Accurate and reliable representations of the external world by the central nervous system depend on the congruous association of pre-receptor, receptor and neuron circuitry mechanisms. In the rostral region of *G. carapo*, there is a high concentration of various types of electroreceptor contained within some sort of 'fovea–parafovea', specialised portions of the skin. This array of highly concentrated electroreceptors projects onto a large area of the electrosensory lobe through two main nerves: the mandibular nerve and the supraorbital nerve. It should be noted that the mandibular nerve is the thickest nerve in *G. carapo*.

Since no elaborate pre-receptor structures have been described in the skin of electric fish, pre-receptor processing has not received particular attention. However, our studies have revealed that the geometry of the body of the fish, specific to gymnotoid species, together with the high conductivity of the tissues of the fish are able to modify the flow of neighbouring currents. We have discovered a 'funnelling effect' that enhances both reafferent and exafferent signals by directing currents towards the fovea and the parafovea. These findings stress the importance of pre-receptor processing for enhancing signals. The current-funnelling effect can be considered analogous to other pre-receptor signal-enhancing mechanisms present in a variety of sensory systems; e.g. the lever action of the bony chain in the middle ear and the light-gathering action of the lens of the vertebrate eye guiding light to the photoreceptor layer.

The internal tissue conductivity causes the fish body to act as a low-resistance path (with the consequent funnelling of currents). Similar mechanisms have been explored and discussed by Kalmijn (1974); however, he postulated that the skin of the fish had a high resistance, a feature that was not found in *G. carapo* (Caputi and Budelli, 1995). The elongated shape of the fish channels the flow of current along its longitudinal axis. In addition, a 'tip effect' induces maximal current densities at the peri-oral region, where the largest concentration of electroreceptors occurs. The present results confirmed the predictions of realistic models stressing the filtering properties of the fish body as a pre-receptor signal conditioner of self-generated signals (Caputi and Budelli, 1995).

Exafferent electrical signals are also enhanced at the foveal region by 1.3- to 4.5-fold, depending on the size of the emitter fish and the distance between the emitter and receptor fish. Furthermore, the experiments substituting the fish with an iron bar showed that signal enhancement is determined only by the high conductance and the peculiar geometry of the fish's body. This effect should facilitate the detection of any kind of electrogenic source (conspecifics, electrogenic predators and myogenic and cardiogenic electrical activity).

It is important to emphasise that there is another effect resulting from pre-receptor processing of self-generated signals. Similar to the findings reported in wave-type electric fish (Rasnow and Bower, 1996), we found that the self-generated field vectors rotate in the caudal parts of the body, but their angles remain constant at the fovea (Fig. 7). In addition, we confirmed the observation of Scheich and Bullock (1974) that fields in the head region are oriented perpendicular to a tangent to the skin surface. Thus, in the head region, there is a sort of 'vector-collimating phenomenon' that causes the LEOD to be oriented in the most efficient direction for stimulating electroreceptors.

This 'collimating phenomenon' results both from the passive properties of the body of the fish and from the relative position of its electric organ. Previous results indicated that the electric organ produces different regional EOD waveforms. Each wave component results from the activation of a set of electrocytes (defined by their membrane properties and innervation pattern) that occupies a specific location within the electric organ (Trujillo-Cenóz et al., 1984; Trujillo-Cenóz and Echagüe, 1989; Macadar et al., 1989; Caputi et al., 1989; Caputi, 1999). For a given point on the trunk, the direction of the field generated by different EOD wave components depends on the relative position of the generating structures with respect to the recording point. Therefore, in the present study on *G. carapo*, large changes in vector angle were detected on the trunk during the EOD. In contrast, and consistent with the fact that the head lacks electrogenic tissues in this species, the local waveform on the head had the same vector angle throughout the EOD. Only the magnitude and sign of the signal varied over time, indicating that the angles of current density vectors were virtually constant at the fovea.

It is pertinent to relate some of our observations on *G. carapo* with general behavioural patterns and common features in sensory biology. First, as may be expected for an active predator, the electroreceptive fovea has evolved close to the mouth in this species. Second, the electroreceptors are arranged within two mosaics that exhibit striking density differences. Consequently, at the first peripheral neural level, the electric image is represented twice, once by a high-resolution low-sensitivity array and once by a low-resolution, high-sensitivity array of electroreceptors. The high-resolution array is linked to the so-called 'slow electrosensory pathway', while the 'low-resolution' array of electroreceptors forms the origin of the so-called 'fast electrosensory pathway'. Previous anatomical/functional studies of the electrosensory fibre projection patterns in *G. carapo* (Castelló et al., 1998) revealed that, at the level of the electric lobe, there is segregation of electrosensory inputs. Afferent fibres integrating the fast electrosensory pathway project by means of calyx-type endings onto spherical cells lying in the rostral regions of the lobe that, in turn, project onto the magnocellularis nucleus. This is a low-resolution pathway (spatially imprecise) with relatively few cells, conveying precise timing signals. In contrast, there is another high-resolution pathway (spatially precise) projecting mainly onto the widely distributed pyramidal cells that, in turn, project onto the torus semicircularis. In this pathway, temporal information seems to be less precise (Shumway, 1989a). It is important to recall, however, that there is some ultrastructural evidence indicating that the two pathways are not completely separated and that precise timing cues can be incorporated into the circuitry that processes precise spatial information (Mathieson et al., 1987).

The decrease in electroreceptor density that accompanies fish growth may be understood in terms of changing requirements for prey detection. Smaller fish require greater resolution from their electrosensory system to enable them to detect smaller prey (usually minute worms and insect larvae). However, a predatory 80 cm long *G. carapo* will typically tackle much larger prey items that can be accurately represented by a lower-density array of electroreceptors.

We gratefully acknowledge the partial support of this research by the Premio Clemente Estable 4014 and PEDECIBA (doctoral fellowship to P.A.A.).

References

Bastian, J. (1986). Electrolocation: behavior, anatomy and physiology. In *Electroreception* (ed. T. H. Bullock and W. Heiligenberg), pp. 577–612. New York: Wiley.

Budelli, R. and Caputi, A. A. (2000). The electric image in weakly electric fish: perception of objects of complex impedance. *J. Exp. Biol*. **203**, 481–492.

Bullock, T. H. (1982). Electroreception. *Annu. Rev. Neurosci.* **5**, 121–70.

Caputi, A. A. (1999). The electric organ discharge of pulse gymnotiforms: the transformation of a simple impulse into a complex temporal electromotor pattern. *J. Exp. Biol.* **202**, 1229–1241.

Caputi, A. and Budelli, R. (1995). The electric image in weakly electric fish. I. A data-based model of waveform generation in *Gymnotus carapo*. *J. Comput. Neurosci.* **2**, 131–147.

Caputi, A. A., Budelli, R., Grant, K. and Bell, C. C. (1998). The electric image in weakly electric fish: physical images of resistive objects in *Gnathonemus petersii*. *J. Exp. Biol*. **201**, 2115–2128.

Caputi, A., Macadar, O. and Trujillo-Cenóz, O. (1989). Waveform generation in *Gymnotus carapo*. III. Analysis of the fish body as an electric source. *J. Comp. Physiol*. A **165**, 361–370.

Carazzi, D. and Levi, G. (1916). *Técnica Microscópica*. Milano: Società Editrice Libraria.

Castelló, M. E., Caputi, A. A. and Trujillo-Cenóz, O. (1998). Structural and functional aspects of the fast electrosensory pathway in the electrosensory lateral line lobe of the pulse fish *Gymnotus carapo*. *J. Comp. Neurol*. **401**, 549–563.

Echagüe, A. and Trujillo-Cenóz, O. (1980). Innervation patterns in the tuberous organs of *Gymnotus carapo*. *Adv. Physiol. Sci*., vol. 31. In *Sensory Physiology of Aquatic Lower Vertebrates* (ed. T. Szabó and G. Czéh), pp. 29–40. Budapest: Pergamon Press.

Heiligenberg, W. and Dye, J. (1982). Labelling of electroreceptive afferents in a gymnotoid fish by intracellular injection of HRP: the mystery of multiple maps. *J. Comp. Physiol.* **148**, 287–296.

Kalmijn, J. (1974). The detection of electric fields from inanimate and animate sources other than electric organs. In *Handbook of Sensory Physiology*, vol. III/3 (ed. A. Fessard), pp. 13–58. Berlin: Springer-Verlag.

Macadar, O., Lorenzo, D. and Velluti, J. C. (1989). Waveform generation of the electric organ discharge in *Gymnotus carapo*. II. Electrophysiological properties of single electrocytes. *J. Comp. Physiol.* A **165**, 353–360.

Mathieson, W. B., Heiligenberg, W. and Maler, L. (1987). Ultrastructural studies of physiologically identified electrosensory afferent synapses in the gymnotiform fish *Eigenmannia*. *J. Comp. Neurol.* **255**, 530–537.

Ramón y Cajal, S. and de Castro, F. (1933). *Elementos de Técnica Micrográfica del Sistema Nervioso*. Barcelona: Salvat (reprinted in 1972).

Rasnow, B. and Bower, J. M. (1996). The electric organ discharges of the gymnotiform fishes. I. *Apteronotus leptorhynchus*. *J. Comp. Physiol.* A **178**, 383–396.

Scheich, H. and Bullock, T. H. (1974). The detection of electric fields from electric organs In *Handbook of Sensory Physiology*, vol. III/3 (ed. A. Fessard), pp. 201–257. Berlin: Springer-Verlag.

Shumway, C. (1989a). Multiple electrosensory maps in the medulla of weakly electric gymnotiform fish. I. Physiological differences. *J. Neurosci*. **9**, 4388–4399.

Shumway, C. (1989b). Multiple electrosensory maps in the medulla of weakly electric gymnotiform fish. II. Anatomical differences. *J. Neurosci*. **9**, 4400–4415.

Szabo, T. (1965). Sense organs of the lateral line system in some electric fish of the Gymnotidae, Mormyridae and Gymnarchidae. *J. Morph*. **117**, 229–250.

Szabo, T. (1974). Anatomy of the specialised lateral line organs of electroreception. In *Handbook of Sensory Physiology*, vol. III/3 (ed. A. Fessard), pp. 13–58. Berlin: Springer-Verlag.

Szabo, T., Sakata, H. and Ravaille, M. (1975). An electrotonically coupled pathway in the central nervous system of some teleost fish, Gymnotidae and Mormyridae. *Brain Res.* **95**, 459–574.

Trujillo-Cenóz, O. and Echagüe, J. A. (1989). Waveform generation of the electric organ discharge in *Gymnotus carapo*. I. Morphology and innervation of the electric organ. *J. Comp. Physiol.* A **165**, 343–351.

Trujillo-Cenóz, O., Echagüe, J. A. and Macadar, O. (1984). Innervation pattern and electric organ discharge waveform in *Gymnotus carapo*. *J. Neurobiol*. **15**, 273–281.

Viancour, T. A. (1979). Peripheral electrosense physiology: A review of recent findings. *J. Physiol., Paris* **75**, 321–333.

Watson, D. and Bastian, J. (1979). Frequency response characteristics of electroreceptors in the weakly electric fish *Gymnotus carapo*. *J. Comp. Physiol.* A **134**, 191–202.

Westby, G. W. M. (1975). Has the latency dependent response of *Gymnotus carapo* to discharge-triggered stimuli a bearing on electric fish communication? *J. Comp. Physiol*. **96**, 307–341.

Yager, D. D. and Hopkins, C. C. (1993). Directional characteristics of tuberous electroreceptors in the weakly electric fish, *Hypopomus* (Gymnotiformes). *J. Comp. Physiol.* A **143**, 401–414.

Zakon, H. H. (1986). The electroreceptive periphery. In *Electroreception* (ed. T. H. Bullock and W. Heiligenberg), pp. 577–612. New York: Wiley.